

# Functionally Defined White Matter Reveals Segregated Pathways in Human Ventral Temporal Cortex Associated with Category-Specific Processing

## Highlights

- Face- and place-selective regions are associated with separate white-matter pathways
- Diffusion near face- and place-selective regions predicts face and place processing
- Face-blind adults present with atypical white matter near face-selective cortex

## Authors

Jesse Gomez, Franco Pestilli, ..., Jennifer Yoon, Kalanit Grill-Spector

## Correspondence

[gomezj@stanford.edu](mailto:gomezj@stanford.edu)

## In Brief

Gomez et al. reveal separate, parallel fiber tracts in human ventral temporal lobe that support visual processing of faces and places. Subjects with developmental prosopagnosia (face blindness) are shown to have selective disruption of fibers associated with regions processing faces.



# Functionally Defined White Matter Reveals Segregated Pathways in Human Ventral Temporal Cortex Associated with Category-Specific Processing

Jesse Gomez,<sup>1,\*</sup> Franco Pestilli,<sup>2</sup> Nathan Witthoft,<sup>3</sup> Golijeh Golarai,<sup>3</sup> Alina Liberman,<sup>4</sup> Sonia Poltoratski,<sup>5</sup> Jennifer Yoon,<sup>6</sup> and Kalanit Grill-Spector<sup>1,3,7</sup>

<sup>1</sup>Neurosciences Program, Stanford University School of Medicine, Stanford, CA 94305, USA

<sup>2</sup>Department of Psychological and Brain Sciences, University of Indiana, Bloomington, IN 47405, USA

<sup>3</sup>Psychology Department, Stanford University, Stanford, CA 94305, USA

<sup>4</sup>Helen Wills Neuroscience Institute, University of California, Berkeley, Berkeley, CA 94720, USA

<sup>5</sup>Psychology Department, Vanderbilt University, Nashville, TN 37325, USA

<sup>6</sup>Psychology Department, New York University, New York, NY 10012, USA

<sup>7</sup>Stanford Neurosciences Institute, Stanford University, Stanford, CA 94305, USA

\*Correspondence: [gomezj@stanford.edu](mailto:gomezj@stanford.edu)

<http://dx.doi.org/10.1016/j.neuron.2014.12.027>

## SUMMARY

It is unknown if the white-matter properties associated with specific visual networks selectively affect category-specific processing. In a novel protocol we combined measurements of white-matter structure, functional selectivity, and behavior in the same subjects. We find two parallel white-matter pathways along the ventral temporal lobe connecting to either face-selective or place-selective regions. Diffusion properties of portions of these tracts adjacent to face- and place-selective regions of ventral temporal cortex correlate with behavioral performance for face or place processing, respectively. Strikingly, adults with developmental prosopagnosia (face blindness) express an atypical structure-behavior relationship near face-selective cortex, suggesting that white-matter atypicalities in this region may have behavioral consequences. These data suggest that examining the interplay between cortical function, anatomical connectivity, and visual behavior is integral to understanding functional networks and their role in producing visual abilities and deficits.

## INTRODUCTION

The human ventral temporal cortex (VTC) contains spatially segregated regions that process faces (Kanwisher et al., 1997; Weiner and Grill-Spector, 2010) and places (Aguirre et al., 1998; Epstein and Kanwisher, 1998). These regions have been linked to the perception of stimuli from these categories, as responses are higher when these stimuli are perceived as compared to when they are present but not perceived (Allison et al., 1994; Grill-Spector et al., 2004; Moutoussis and Zeki, 2002; Tong et al., 1998), and perturbing responses in these regions by electrical stimulation disrupts perception (Allison

et al., 1994; Mégevand et al., 2014; Parvizi et al., 2012; Rangarajan et al., 2014). These category-selective regions follow a regular arrangement relative to cortical folding: the midfusiform sulcus (MFS) predicts the location of face-selective regions (Weiner et al., 2014; Weiner and Grill-Spector, 2010) as well as cytoarchitectonic regions in the fusiform gyrus (FG; Weiner et al., 2014), and the collateral sulcus (CoS) predicts the location of place-selective regions (Nasr et al., 2011; Weiner and Grill-Spector, 2010). This orderly organization suggests that anatomical factors such as white-matter connectivity may also constrain this functional topology (Tallinen et al., 2014; Zeki and Shipp, 1988). However, the role of white matter in perceptual processing and in shaping the functional topology of VTC is not as well understood.

Diffusion-weighted imaging (DWI) combined with tractography has been used to examine the organization of white matter in the ventral temporal lobe (VTL) and its role in behavior. Several studies have reported that properties of the inferior longitudinal fasciculus (ILF), a large white-matter tract interconnecting the occipital and temporal lobes, are correlated with behavior. However, findings vary with respect to the behavior that is coupled with ILF diffusion properties, as well as the direction of the correlation. For example, Thomas et al. (2008) reported that typical subjects have higher FA in the ILF than developmental prosopagnosic (DP) subjects, while Tavor et al. (2014) found that lower values of FA in typical subjects are associated with better face recognition. Other studies report that the FA of the ILF also correlates negatively with reading ability (Yeatman et al., 2012a) and recognition memory of places (Tavor et al., 2014) but correlates positively with social cognition (De Pisapia et al., 2014) and pitch perception (Dohn et al., 2013).

The apparently nonspecific role of the ILF in a variety of behaviors may not be surprising, considering the ILF is a large fasciculus reaching up to 12cm in length. This white-matter highway courses from the occipital lobe to the temporal lobe (Catani et al., 2003), passing along its extent early, intermediate, and high-level visual regions, any one of which may be a rich source of contributory projections (Figure 1A). Although it is clear from prior studies that the ILF is important for behavior, understanding of how white matter relates to functional regions or

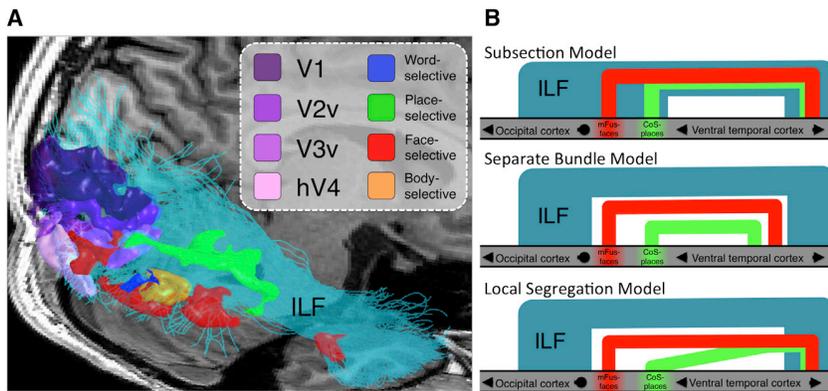


**Figure 1. The Inferior Longitudinal Fasciculus Traverses Many Functional Regions of Interest in the Occipital and Temporal Lobes**

(A) An example ILF (cyan) in the right hemisphere of an adult passes many fROIs including low-level (V1-hV4) regions in the occipital lobe to high-level category-selective regions in ventral temporal cortex (VTC). These fROIs are by no means an exhaustive list of regions connecting to the ILF, further underscoring the nature of the ILF as a large axonal highway relaying information between the occipital and temporal lobes.

(B) Three possible organizations of functionally defined white matter (FDWM) connecting place- or face-selective cortex (green and red, respectively) to the anterior temporal lobe relative to the ILF (blue). (Top) Subsection model—mFus-fibers and

CoS-fibers are overlapping subsets of the core ILF. (Middle) Separate tract model—mFus- and CoS-fibers are parallel tracts separate from the ILF. (Bottom) Local segregation model—mFus- and CoS-fibers are spatially distinct close to functional regions and partially converge in the anterior temporal lobe.

relays category-specific information is limited through such large-scale investigations.

Recent studies have examined white matter in the occipital and temporal lobes at a finer scale, with results suggesting the existence of specific white-matter connections associated with face- and place-selective regions. Gschwind, Pyles, and colleagues reported higher connectivity among face-selective regions compared to surrounding cortex (Gschwind et al., 2012; Pyles et al., 2013). Additionally, Saygin and colleagues showed that unique white-matter connectivity fingerprints differentiate face- and place-selective regions in VTC (Saygin et al., 2012). These findings suggest that face- and place-selective regions communicate through separable white-matter pathways. However, the relationship of these fine-scale tracts to behavior and to large-scale fasciculi such as the ILF remains unclear.

While structure and function are likely inextricable in the organization of VTC, we address two open questions in this paper. First, what is the anatomical arrangement of white-matter tracts in the VTL associated with category-specific regions? Second, if there are separate tracts for different regions, do their white-matter properties relate to category-specific behavior?

In each subject, we identified white-matter tracts connecting face- or place-selective regions with the anterior temporal (AT) lobe (Figure 2; Wakana et al., 2004). This approach allowed us to examine the arrangement of white-matter tracts relative to cortical anatomy and to the ILF. We explored three possible schemes of white-matter connections associated with functional regions in VTC. Axons associated with face- and place-selective regions may be part of a large interconnected network in the VTL. That is, they may merge with the ILF-like ramps to a highway (Figure 1B, top), consistent with studies showing that the structural properties of the ILF are important for both face and place recognition. Conversely, axons associated with face- and place-selective regions may be parts of segregated networks arranged laterally-medially for face and place processing, respectively, and may remain segregated throughout the VTL (Figure 1B, middle) as suggested by previous findings (Gschwind et al., 2012; Pyles et al., 2013; Saygin et al., 2012). As an intermediate scheme, there may be a lateral-medial segregation of white matter close to functional regions, and convergence of these in

anterior sections of the temporal lobe where associative knowledge combining information across domains is generated (Figure 1B, bottom) (Haskins et al., 2008).

Second, we examined whether diffusion properties of the white matter associated with face- and place-selective regions correlate with category-specific performance in both typical adults and adults with developmental prosopagnosia (DP) (McConachie, 1976). DP is a high-level visual deficit characterized by a specific impairment in recognizing faces despite having normal vision, intelligence, and sociocognitive abilities (Behrmann et al., 2011; Duchaine, 2011). Comparing structure-behavior correlations in DPs versus typical adults allows examination of how these relationships may differ in subjects with deficits in face perception. We used the Benton Face Recognition task (Benton et al., 1983) to assess face processing ability and a scene-recognition memory task (Golarai et al., 2010) to assess place processing ability.

White-matter properties were estimated through DWI, which is sensitive to the diffusion of water. Free-diffusing water in white-matter voxels can be summarized by the degree of directionality of diffusion in a single direction versus all possible directions, known as fractional anisotropy (FA). FA reflects a ratio between axial diffusivity (AD), which is parallel to the main diffusion direction, and radial diffusivity (RD), which is perpendicular (Basser and Pierpaoli, 1996; Beaulieu, 2002). Changes in either RD or AD can affect FA and may have behavioral consequences. For example, FA can increase because of greater diffusion along the main direction (e.g., from tighter axonal spacing), or from lowered diffusion in other directions (e.g., from greater myelination). Either can improve information relay and result in a positive correlation with behavior. A reduction in FA, however, does not necessarily imply compromised axonal properties (Jones, 2008). For instance, if a voxel close to cortex has a main diffusion axis that runs parallel to the cortical surface, then increases in the myelination or number of axons diving into the nearby cortex would actually reduce FA. Thus, a meaningful correlation between FA and behavior can be either positive or negative, and depends not only on the degree of myelination and axon density but also on local environmental factors such as the orientation of axons of interest relative to the main diffusion axis.

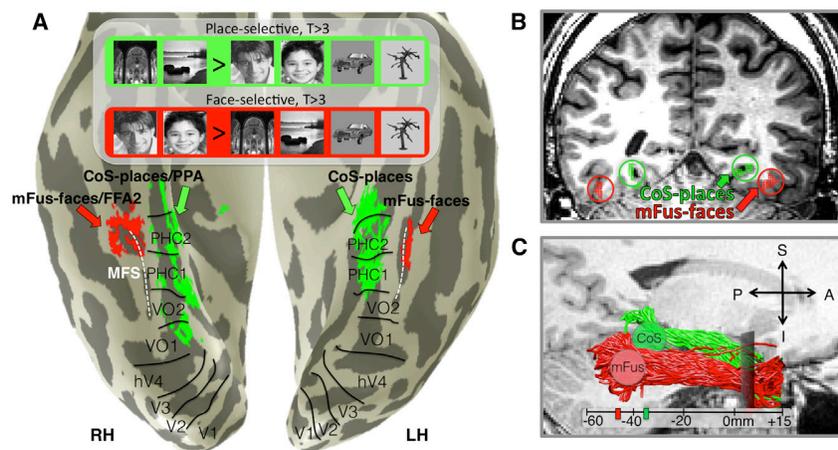


**Figure 2. Functionally Defining White-Matter Tracts by Combining fMRI and DWI**

(A) Example adult cortical surface depicting mFus-faces/FFA-2 (red, faces > places and objects,  $p < 0.001$ , voxel level) and CoS-places/PPA (green, places > faces and objects,  $p < 0.001$ , voxel level). Boundaries of retinotopic regions are indicated in black. Dashed white indicates mid fusiform sulcus (MFS).

(B) A coronal slice from a different example adult indicating mFus-faces/FFA-2, CoS-places/PPA as well as 6 mm spheres extending into white matter that were expanded from the center of each fROI to define mFus- and CoS-fibers.

(C) Functionally defined white matter (FDWM) was defined as all fibers intersecting the spheres as illustrated in (B) with the anterior anatomical plane where the temporal and frontal lobes separated (gray rectangular plane). Resulting mFus- and CoS-fibers of a representative subject with the average location of the mFus and CoS spheres across all subjects marked on the scale bar (zero is anterior commissure).

We also examined the relationship between FA and face and place processing at two spatial scales: the level of the entire tract and the level of white matter local to face- and place-selective regions. Finding that a behavioral measure is associated with fiber properties along the entire length of a tract would suggest that the connectivity between distal cortical regions might be important for that behavior. Alternatively, finding that a behavioral measure is associated with properties of white matter in the local vicinity of a specific functional region would suggest that the local connectivity of that region is likely key to that behavior. Indeed, examining local white-matter properties maximizes the probability of measuring from axons belonging to category-selective neurons in the neighboring cortical sheet.

## RESULTS

### Separate White-Matter Tracts Are Associated with Face- and Place-Selective Regions

We first identified the white-matter tracts associated with regions of VTC selective for faces or places in nine typical adults. We used fMRI and a standard localizer (Golarai et al., 2010) to functionally define in each subject a face-selective region (mFus-faces/FFA-2) on the lateral FG overlapping the anterior tip of the MFS (Weiner et al., 2014; Weiner and Grill-Spector, 2010), and a place-selective region (CoS-places/PPA) medial to mFus-faces on the CoS (Epstein and Kanwisher, 1998; Nasr et al., 2011) (Figure 2A). We then used probabilistic tractography to create a whole-brain connectome in each subject using constrained spherical deconvolution (CSD) (Tournier et al., 2007) to model crossing fibers and track closer to cortex (Experimental Procedures).

Standard practice in tractography is to generate a connectome (Sporns et al., 2005) from diffusion measurements without validating the resulting tracts. We used modern probabilistic fiber-tracking methods (Tournier et al., 2012), which have been shown to more accurately represent human white matter (Pestilli et al., 2014). In addition, we employed a recently developed

method, Linear Fascicle Evaluation (LiFE; see Experimental Procedures), to evaluate our fiber tracking results (Pestilli et al., 2014). LiFE eliminates false alarm fibers and tests the strength of evidence in support of tracts of interest. To do so, LiFE builds a model of diffusion measurements from the candidate probabilistic connectome and then tests how well each fiber predicts the actual diffusion measurements from which the connectome was derived. In doing so, it eliminates the false alarm fibers that do not predict diffusion measurements. Applying LiFE to our data generated an optimized connectome that contained  $40.6\% \pm 1.6\%$  fewer fibers than the candidate connectome.

From the optimized connectome we extracted the white-matter tracts that traverse the VTL from posterior to anterior that intersect with either mFus-faces/FFA-2 or CoS-places/PPA and an anatomical plane in the AT lobe used to define the anterior end of the ILF (see Experimental Procedures; Figure 2C). We refer to these tracts as functionally defined white matter (FDWM), as they are defined based on their intersection with functional regions of interest (fROI). Using this FDWM procedure, we found two white-matter tracts arranged from posterior to anterior along the VTL. One tract was located laterally and inferiorly, intersecting with mFus-faces (mFus-fibers). The other tract was located more medially and superiorly, intersecting with CoS-places (CoS-fibers; Figure 2C). Notably, this medial-lateral separation in the FDWM of face- and place-selective cortex was visible in every subject and hemisphere (Figure 3A).

Because this study identifies mFus- and CoS-fibers, we validated these tracts using a virtual lesion method implemented in LiFE, in which we evaluated the strength of evidence supporting the identified tracts (Experimental Procedures). This is accomplished by examining the effect of a virtual lesion of an identified tract on the ability to predict diffusion measurements in an independent DWI data set. In other words, we (1) computed for both the lesioned and unlesioned connectome a cross-validated root-mean-square error (RMSE) between the diffusion measurements predicted by the connectome model and actual diffusion measurements in a second independent DWI set and

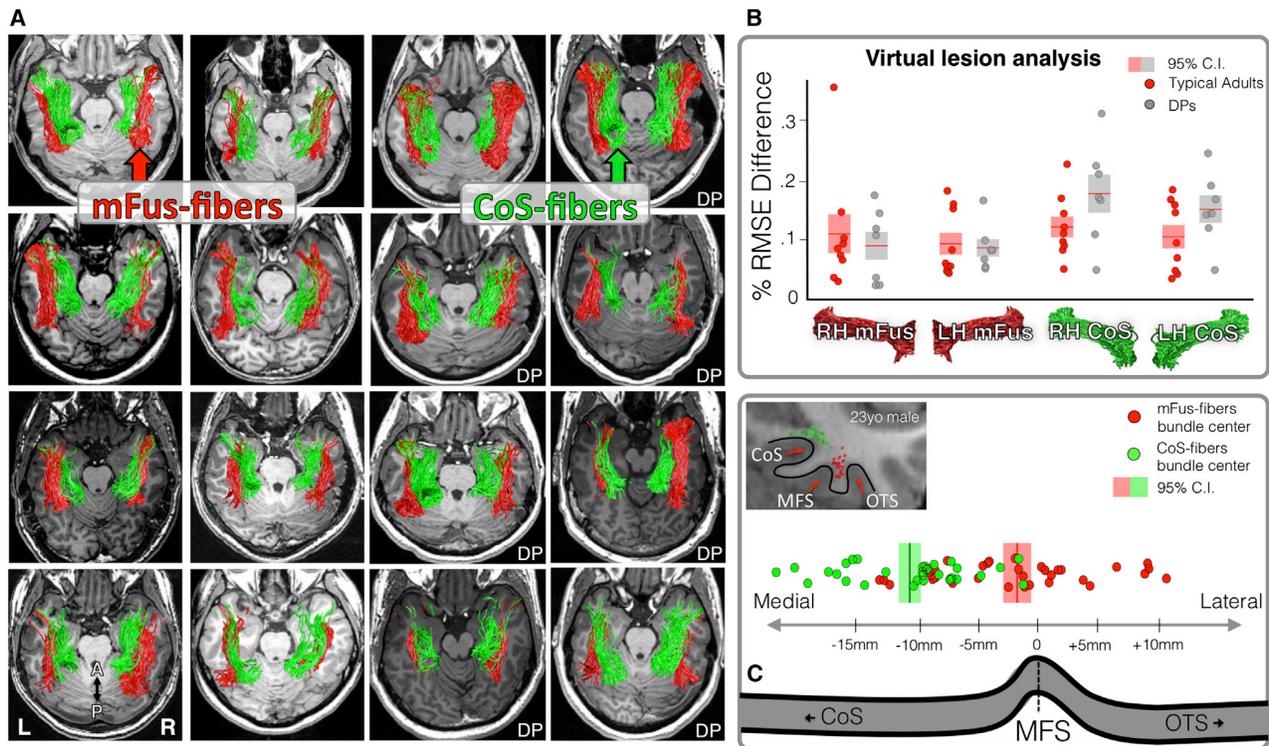


**Figure 3. FDWM mFus- and CoS-Fibers in Individual Subjects**

(A) mFus-fibers (red) and CoS-fibers (green). First nine panels illustrate typical adults from group 1, and the rest are developmental prosopagnosics (DP). (B) Validation of mFus-fibers and CoS-fibers using the virtual lesion method implemented in the linear fascicle evaluation (LiFE) software. Root-mean-square error (RMSE) was significantly lower ( $p < 0.05$ ) when mFus and CoS fiber tracts were included in the connectome model than in the model in which these tracts were virtually lesioned. There were no significant differences between typical adults (red) and DP subjects (gray). Red and gray shaded areas are confidence intervals derived from standard error calculated to 95% confidence. (C) In posterior regions, the bifurcation of the mFus and CoS fiber tracts is systematically arranged relative to the midfusiform sulcus (MFS). (Top) A coronal slice of a typical subject depicting the topology of the CoS, MFS, and occipitotemporal sulcus (OTS). (Bottom) Center of mFus- (red) and CoS-fibers (green) relative to the anterior fundus of the MFS. Each point is a subject.

(2) compared the RMSE of the lesioned and unlesioned connectomes. A positive difference in the RSME between the unlesioned and lesioned model would provide evidence that the unlesioned model is a better model of connectivity. We found that the connectome including mFus-fibers and CoS-fibers had significantly lower RMSE in predicting the diffusion measurements in the second DWI data set than a connectome in which the tracts had been virtually lesioned (Figure 3B). These results indicate that the separate tracts that we identified associated with mFus-faces and CoS-places, respectively, are reliable because they significantly improve modeling the underlying structure of VTL white matter.

The anatomy of mFus- and CoS-fibers shows that they are arranged along an anterior-posterior axis in VTL and are largely nonoverlapping. They formed distinct tracts in their posterior halves, where the percent of shared voxels between each tract was relatively small (mFus-fibers,  $3.2\% \pm 2.1\%$ ; CoS-fibers,  $1.9\% \pm 2.4\%$ ). In their anterior halves, where tracts partially converged, the overlap was more than five times greater (mFus-fibers,  $14.1\% \pm 4.4\%$ ; CoS-fibers,  $12\% \pm 7.8\%$ ). In addition, CoS-fibers were on average 2.8 times closer to cortex

( $2.5 \text{ mm} \pm 1.2 \text{ mm}$ ) than mFus-fibers ( $4.1 \text{ mm} \pm 2 \text{ mm}$ ),  $t(30) = 2.58$ ,  $p = 0.01$ . We found little evidence of white-matter tracts directly connecting mFus-faces to CoS-places. There were no tracts interconnecting mFus-faces and CoS-places in 75% of hemispheres. In the remaining hemispheres, these tracts did not survive crossvalidation testing by LiFE ( $\Delta\text{RMSE}$  not significantly  $> 0$ ; right hemisphere:  $t[3] = 1.4$ ,  $p = 0.17$ ; left hemisphere:  $t[3] = 0.59$ ,  $p = 0.56$ ), suggesting that direct connectivity from mFus-faces to CoS-places may not exist. Interestingly, the bifurcation of mFus-fibers and CoS-fibers was arranged in a consistent manner relative to cortical folding. Tracts associated with mFus-faces pass above the MFS, a sulcus that longitudinally bisects the FG (Weiner et al., 2014), and tracts associated with CoS-places are located 1cm more medially (Figure 3C).

Examining the location of mFus-fibers and CoS-fibers relative to the ILF shows that they lie ventral to, and are largely separate from, the ILF (Figure 4A; Movie S1). We quantified their spatial relationship with respect to the ILF in two ways. First, we calculated the Euclidean center of the ILF by deriving the mean coordinate of its constituent fibers within coronal planes at various nodes along its extent, as well as their spread (standard

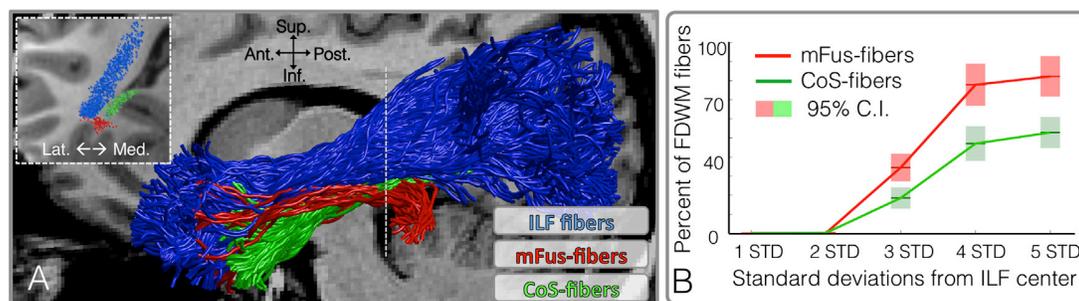


**Figure 4. Arrangement of mFus-Fibers and CoS-Fibers Relative to the ILF**

(A) A typical right ILF (blue) from an example subject alongside the tracts of mFus- (red) and CoS- (green) fibers.

(B) The percentage of mFus- and CoS-fibers encountered as a function of distance from the Euclidean center of the ILF. Of ILF fibers, 95% are within 2 standard deviations (STD) of its center, and 99.7% of the fibers are 3 STD from the center. Shaded areas indicate confidence intervals derived from standard error across subjects calculated to 95% confidence.

deviation). Of the ILF's fibers, 95% lie within 2 SD of its center. However, all mFus- and CoS-fibers are more than 2 SD away from the ILF (Figure 4B). In fact, a majority of mFus-fibers ( $65.5\% \pm 14.8\%$ ) and CoS-fibers ( $81.5\% \pm 11.5\%$ ) are more than 3 SD from the ILF center (Figure 4B). Second, we calculated the percent of FDWM fibers overlapping with voxels that also include ILF fibers. In their posterior third, only  $35.1\% \pm 12.8\%$  of mFus-fibers and  $28.2\% \pm 16.5\%$  of CoS-fibers share voxels with the ILF. In their anterior third, the overlap increases, with  $46.2\% \pm 15.3\%$  of mFus-fibers and  $39.5\% \pm 17.1\%$  of CoS-fibers sharing voxels with the ILF. Together, these analyses reveal that FDWM tracts associated with face- and place-selective regions in VTC are consistent with a local segregation model of connectivity within VTC (Figure 1B, bottom): they are segregated from one another and from the ILF near category-selective regions, partially converge in the AT lobe, and are largely ventral to the ILF.

#### Local FDWM Exhibits a Category-Specific Relationship with Behavior

Using DWI, we next sought to test the hypothesis that properties of white-matter tracts associated with category-selective regions relate to category-specific behavior. We examined this relationship at two spatial scales—white matter local to fROIs (within 10 mm) and the scale of entire mFus- and CoS-fibers tracts. Our data reveal a clear relationship between category-specific performance in typical adults and properties of FDWM local to category-selective fROIs (Figure 5).

First, accuracy on the Benton was positively correlated with FA of FDWM local to mFus-faces in the right hemisphere ( $r[9] = 0.64$ ,  $p = 0.06$ ; Figure 5, top left, red). Because we tested a small number of subjects, we obtained an additional group of subjects to validate these findings. As with the original subjects, in each of the subjects of this new group, we successfully extracted the mFus-faces and CoS-places FDWM tracts (Figure S1). Notably, we found a significantly positive correlation between accuracy on the Benton and FA local to right mFus-faces in the second subject group ( $r[8] = 0.75$ ,  $p < 0.05$ ; Figure 5, top left, dark red), replicating the positive correlation in the first group. Since there were no significant between-group differences in FA values ( $t[15] = 0.2$ ,  $p = 0.85$ ) or Benton scores

( $t[15] = 0.1$ ,  $p = 0.93$ ), we combined all subjects into a single correlation analysis relating Benton accuracy and right mFus-fibers FA, resulting in a significant correlation ( $r[17] = 0.7$ ,  $p = 0.0017$ , Bonferroni-corrected threshold of  $p = 0.05/16 = 0.00313$ ). Further examination revealed that this correlation was driven by AD next to mFus-faces ( $r[17] = 0.7$ ,  $p < 0.005$ ), but not RD ( $r[17] = -0.11$ ,  $p = 0.3$ ). It is also interesting to note that regression coefficients of the Benton-FA correlation extracted from one subject group predicted Benton scores based on FA measurements in the second group. Indeed, a model based on one set of measurement predicts 47% of the variance in the other group, which is comparable to the amount of variance explained by the within-group regression (49%).

Notably, this structure-behavior relationship was specific. There was no significant correlation between the same FA measurements and scene recognition ability (Figure 5, top right;  $r[17] = 0.12$ ,  $p > 0.05$ ). Furthermore, the Benton-FA correlation was significantly higher than the scene recognition-FA correlation (Fisher transform,  $p < 0.01$ ).

We also found a significant negative correlation between place processing and FA in FDWM local to left CoS-places. This correlation was significant in each of the subject groups (Figure 5, bottom right). While there was a significant between-group difference in the average FA of the fibers local to left CoS-places ( $t[15] = 2.85$ ,  $p = 0.01$ ), there was also a significant between-group difference in scene recognition scores ( $t[15] = 2.23$ ,  $p = 0.04$ ). Thus, when combining all subjects into a single pool, the correlation between FA local to left CoS-fibers and scene recognition became more significant ( $r[17] = -0.75$ ,  $p = 0.0004$ , Bonferroni-corrected threshold 0.00313). Here, the correlation between place processing and FA was driven largely by RD ( $r[17] = 0.6$ ,  $p = 0.27$ ) compared to AD ( $r[17] = -0.21$ ,  $p = 0.35$ ). Examining how well this relationship can predict data in an independent set, we found that regression coefficients from one group of subjects explained 16% of the variance in the second group of subjects, which is about a third of variance (50%) explained by the within-group regression models.

In contrast, there was no significant correlation between the FA local to CoS-places and face processing ( $r[18] = -0.07$ ,

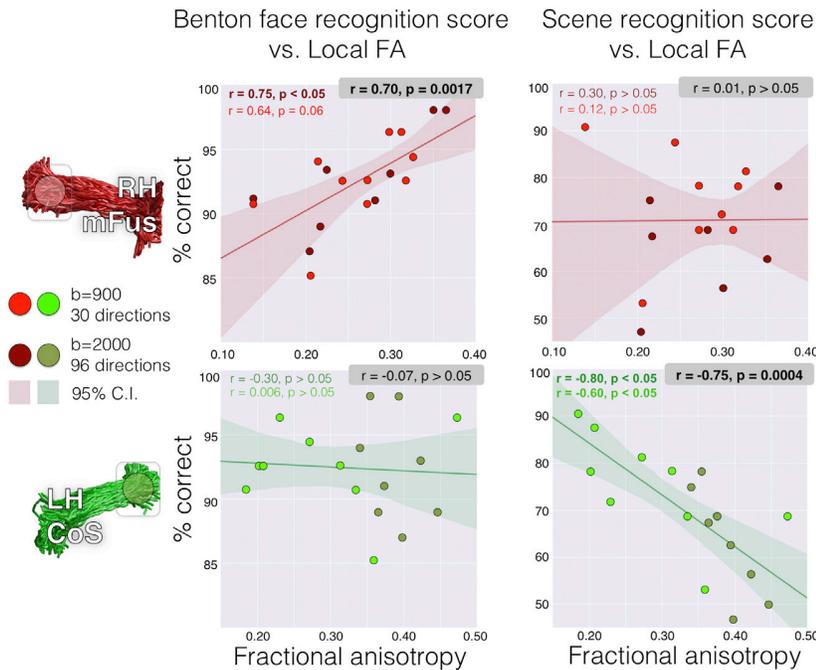


**Figure 5. Correlations between the Fractional Anisotropy of Local FDWM Voxels and Performance in Face- and Place-Processing Tasks in Typical Adults**

Each point represents a subject's performance on a behavioral task versus mean FA of local FDWM (within 10 mm) centered above a fROI. Red dots indicate FDWM local to mFus-faces/FFA-2 in the right hemisphere; green dots indicate FDWM local to CoS-places/PPA in the left hemisphere. Group 1 subjects are shown in lighter colors, and group 2 subjects are shown in darker colors. Correlation results combining both groups are reported in black, and results within each group are reported in their respective group colors. Solid lines indicate the line of best fit for each FDWM-behavior correlation using all subjects. Shaded areas indicate 95% confidence intervals derived from bootstrapping.

$p = 0.79$ ; Figure 5, bottom left). Furthermore, the correlation between FA in left CoS-fibers and scene recognition was significantly different than the correlation between the same FA and Benton scores (Fisher transform,  $p < 0.01$ ). No other correlations between FA and behavior were significant; these remaining correlations are reported in Table S1.

We next examined whether or not the diffusion properties of entire tracts also predict behavior by averaging FA over the entire mFus-fibers, CoS-fibers, or ILF in each hemisphere. While the whole left CoS-fibers tract correlated significantly with scene processing ( $r[17] = -0.67, p = 0.003$ ), we found no other significant correlations between behavior and white-matter properties across entire FDWM tracts. In addition, properties of the ILF had no significant correlation with behavior (Table S1). These results suggest that the white-matter local, and the tracts specific, to a category-selective region are better predictors of category-specific behaviors rather than the average properties of a large fasciculus. This may in turn suggest that individual differences in the input/output projections of cortical regions processing faces and places are behaviorally relevant.

#### Atypical FDWM-Behavior Relationship in DPs Near Face-Selective Cortex

Given the observation of a specific relationship between white matter and behavior, a strong test of this hypothesis would be to examine this relationship in a group of subjects with a selective perceptual deficit. Thus, we repeated these measurements in a group of DPs. We examined three possible outcomes in which DPs could deviate from typical adults: (1) FDWM tracts in the VTL of DPs may be qualitatively different, i.e., absent or abnormal in their anatomy; (2) there may be quantitative differences in diffusion properties of FDWM tracts between DPs and typical adults; and (3) there may be quantitative differences

between DPs and typical adults in the correlation between face processing and FDWM local to face-selective regions.

We identified eight adults with DP as assessed by the Cambridge Face Memory Test (CFMT) (Duchaine and Nakayama, 2006). DPs scored  $55.6\% \pm 10.9\%$  (mean  $\pm 1$  SD) on the CFMT, which was significantly ( $t[14] = 6.9, p < 0.0001$ ) lower than the scores of the typical adults ( $90.8\% \pm 9.5\%$ ; Figure S2). In every DP subject we localized category-selective mFus-faces and CoS-places fROIs in each hemisphere and defined FDWM tracts associated with mFus-faces/FFA-2 and CoS-places/PPA (as in Figure 2). The functional topology of category-selective responses was the same in DPs and typical adults. Like in typical subjects, face-selective activations in DPs were located on the lateral FG, with a cluster overlapping the MFS, and place-selective responses were found in the CoS. In DPs, mFus-faces were significantly smaller compared to typical adults bilaterally ( $F[1.48] = 18.66, p < 0.0005$ ), but there were no significant differences across groups in the size of CoS-places ( $F[1.48] = 3.02, p > 0.05$ ).

We found no qualitative differences in FDWM tracts associated with face- and place-selective regions between DPs and typical adults. As in typical adults, we found separate tracts organized posterior to anterior associated with mFus-faces and CoS-places, which converged in the AT lobe (Figure 3A). Using LiFE we found that these FDWM explained a significant amount of variance of the diffusion data in an independent data set (Figure 3B), indicating that they are valid tracts.

We found, however, quantitative differences between DPs and typical adults in the diffusivity of mFus-fibers. Because changes in DWI sequences can affect the apparent diffusivity constants measured (AD, RD) more than their ratio (FA), we compare these metrics across DP subjects and typical adults for data that were collected on the same scanner using the same DWI sequence. For each diffusivity measure, we performed an analysis of variance (ANOVA) comparing DP and typical adults locally and across whole FDWM tracts. For any F-statistic that passed a Bonferroni-corrected threshold of  $0.05/6 = 0.008$ , we computed

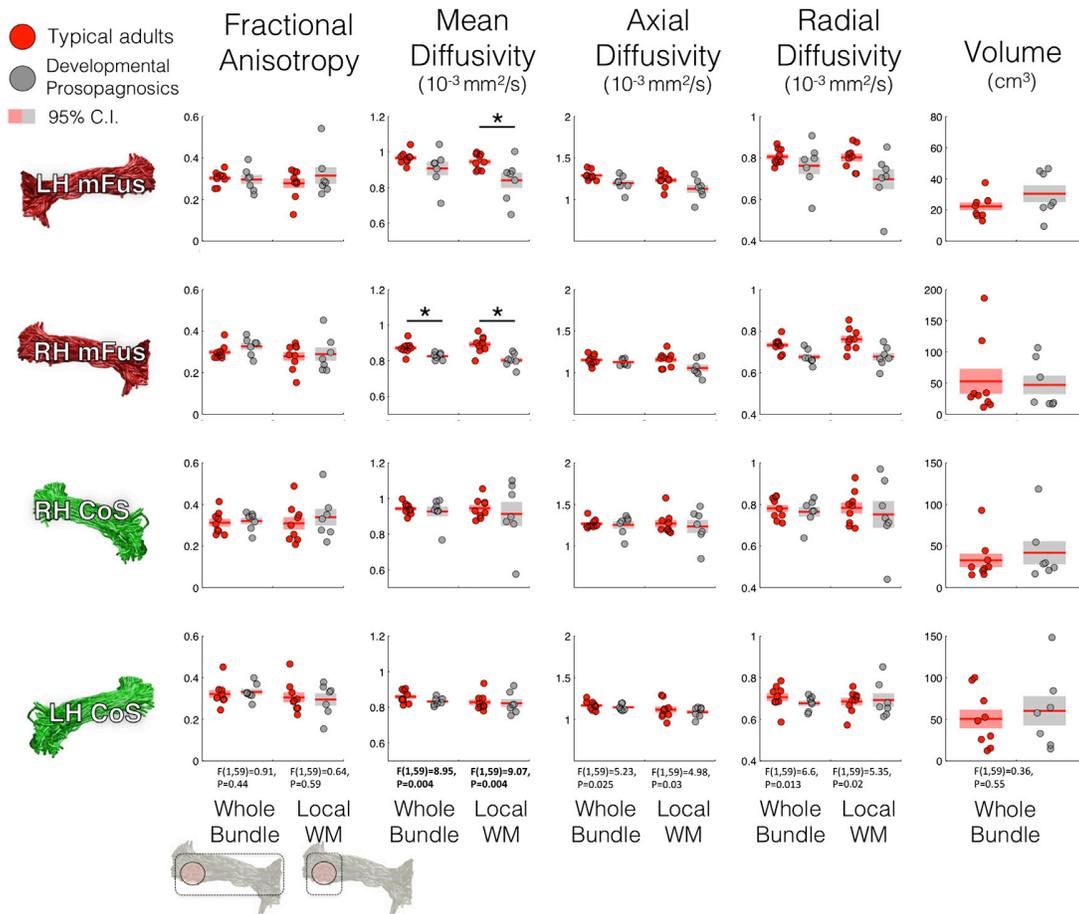


**Figure 6. White-Matter Characteristics in Typical and DP Adults**

White-matter properties measured by average fractional anisotropy (FA), mean diffusivity (MD), AD, and RD are shown for FDWM local to fROIs (right columns) and averaged across entire FDWM tracts (left columns). Volume (cm<sup>3</sup>): volume of voxels occupied by a FDWM tract. Each row is a different fiber tract. Red indicates typical adults; gray indicates DPs; horizontal bold red line indicates group mean; shaded areas indicate 95% confidence intervals. Two-way ANOVAs with factors of group and tract comparing DP and typical adults were conducted per white-matter property separately for whole tracts and local tracts. Asterisks indicate significant differences between typical and DP adults based on t tests, performed if the ANOVA was significant (bolded).

a t test to assess if properties of a tract significantly varied across DPs and typical adults. DP subjects demonstrate lower mean diffusivity (MD) values in the mFus-fibers tract locally in both hemispheres (right,  $t[14] = 3.95, p = 0.001$ ; left,  $t[14] = 2.5, p = 0.02$ ) and across the whole mFus-fibers tract in the right hemisphere ( $t[14] = 3.95, p = 0.007$ ) (Figure 6). Such diffusivity differences were not visible in CoS-fibers. There were also no significant between-group differences in (1) other diffusivity measures, (2) the volume of CoS- or mFus-fibers ( $F(1,59) = 0.36, p = 0.55$ ), or (3) the volume of the ILF ( $ts < 1.6, ps > 0.13$ ). Importantly, differences in diffusivity patterns cannot be attributed to differences in the SNR of DWI data, with no significant difference in the non-diffusion-weighted images of DP and typical adult data sets ( $t[14] = 0.82, p = 0.42$ ; Figure S2).

Focusing on the relationship between FA and behavior, the Benton-FA correlation in DPs was significantly different from the correlation in typical adults (Fisher transform,  $p = 0.01$ ; Figure 7A) and showed a negative trend ( $r[8] = -0.5, p = 0.2$ ). This

atypical correlation between behavior and white matter was restricted to mFus-faces, as DPs demonstrated no significant differences compared to typical adults in any other correlations (Fisher transform,  $p > 0.05$ ; see Table S1). To verify that this atypical structure-behavior relationship in DP is associated with deficits in face processing more generally, we examined if this differential relationship extends to another test of face processing: the CFMT. Again, we observe in typical adults a significantly positive correlation between CFMT scores and FA local to mFus-faces ( $r[15] = 0.71, p < 0.003$ ; Figure 7B). Additionally, this correlation was significantly different than the FA-CFMT correlation in DPs (Fisher transform,  $p = 0.04$ ; Figure 7B), who instead exhibit a negative trend.

Overall, comparing DPs to typical adults revealed no qualitative differences in VTL white-matter tracts associated with face or place processing, but instead revealed significant differences in the MD and the structure-behavior relationship specifically in white-matter local to mFus-faces.

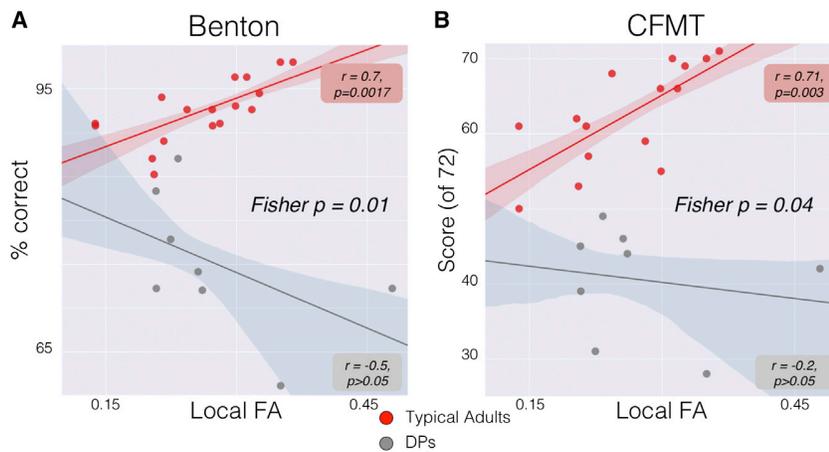


**Figure 7. Correlations between the Fractional Anisotropy of Local FDWM Voxels and Performance in Face-Processing Tasks in DPs and Typical Adults**

(A) Each point represents a subject's performance on the Benton face recognition task versus mean FA of FDWM voxels local to of right mFus-faces/FFA-2. Solid lines indicate the line of best fit plotted for DPs (gray) and typical adults (red). Shaded areas indicate 95% confidence intervals derived from bootstrapping. The Fisher transform indicates a significant difference among correlations in typical adults and DPs.

(B) Same as (A), but for CFMT scores.

## DISCUSSION

### The Interplay between Structure, Function, and Behavior

Our data suggest that properties of white matter either local or specific to a fROI, rather than properties of entire fasciculi, can have a category-specific relationship to behavior. We found that white-matter properties local to mFus-faces in the right hemisphere specifically correlated with face-processing ability and that white-matter properties of fibers interconnecting CoS-places in the left hemisphere were significantly correlated with place-processing ability. These findings are in line with the observation that face-selective regions are directly involved in the perception of faces (Parvizi et al., 2012; Rangarajan et al., 2014) and place-selective regions with the perception of places (Mégevand et al., 2014; Tong et al., 1998). Importantly, our findings extend this relationship into the neighboring white matter.

Notably, the correlations between FA in mFus-fibers and behavior were observed in the right hemisphere, where dominance for face processing has been suggested by larger size (Allison et al., 1994; Golarai et al., 2007; Kanwisher et al., 1997; Yovel et al., 2008), higher probability of occurrence (Peelen and Downing, 2005; Weiner and Grill-Spector, 2010), and higher anatomical localization consistency of face-selective regions (Weiner et al., 2014) compared to the left. FA of left CoS-fibers was correlated with scene-recognition ability both locally and across the entire CoS-fibers tract. This may imply that not only local connections to CoS-places but also distal connections between the CoS-places and the AT lobe are important for scene recognition. Together, these results advance previous research linking white-matter properties of the ILF to behavior (Tavor et al., 2014) in that they (1) substantially increase the spatial resolution of measurements linking the role of white matter in behavior by an order of magnitude, (2) specify the source of behaviorally predictive white matter to those connections local and specific to functionally selective cortex, and (3) suggest that white matter associated with a particular cortical region is a better predictor of behavioral abilities than properties of large fasciculi.

The physiological factors underlying the diffusivity properties of our reported fiber tracts are likely diverse (Beaulieu, 2002)

and difficult to directly link to microscopic tissue properties (Jones et al., 2013).

Since we found a correlation between behavior and local white matter properties that is opposite in sign between mFus-faces and CoS-places, it may be useful to consider the orientation of the white matter relative to these cortical regions and its influence on the sign of the observed correlations (Figure 8). MFus-faces lies on the crown of a gyrus (Figure 2B), where tractography close to cortex is difficult due to axons fanning sharply into the surrounding cortical walls (Jbabdi and Johansen-Berg, 2011; McNab et al., 2013). Consequently, resultant tracts may be well aligned but further from cortex, therefore containing relatively fewer axons oriented toward gyral walls (Figure 8). Here, one might hypothesize that increased local connectivity would increase FA. The situation may be reversed near CoS-places, which rests in a fundus (Figure 2B). The CoS is relatively exposed to longitudinal tracts in the temporal lobe, which travel parallel and close to cortex (Figure 8). Here, one might hypothesize that increased local connectivity into CoS-places (more diving axons) would reduce FA. In line with this hypothesis, we observed that the distance between the fROI and the center of the FDWM tract immediately superior to it was significantly greater in mFus-fibers than CoS-fibers. Given that in typical adults the correlation between face processing and FA was due to the local AD, our data suggest the possibility that properties of axons that are aligned with mFus-fibers (such as axon quantity or myelination) may be relevant to face processing. However, in CoS-fibers, the correlation between behavior and FA was negative, and largely driven by RD, suggesting the possibility that properties of axons perpendicular to CoS-fibers, or those oriented toward cortex, may be relevant for place processing. Future experiments using higher-resolution DWI (McNab et al., 2013) or postmortem brains (Axer et al., 2011) can elucidate the direction of fibers diving into cortex relative to the dominant diffusion direction in a voxel and test these hypotheses.

### Atypical Development of the Structure-Function Relationship and Behavioral Deficits

Supporting the idea that visual behavior relies on both the processing in a functional region and its connectivity were the striking differences in FDWM properties of subjects with face-processing deficits. While DP subjects had the same large-scale organization of white-matter tracts in the VTL as typical subjects

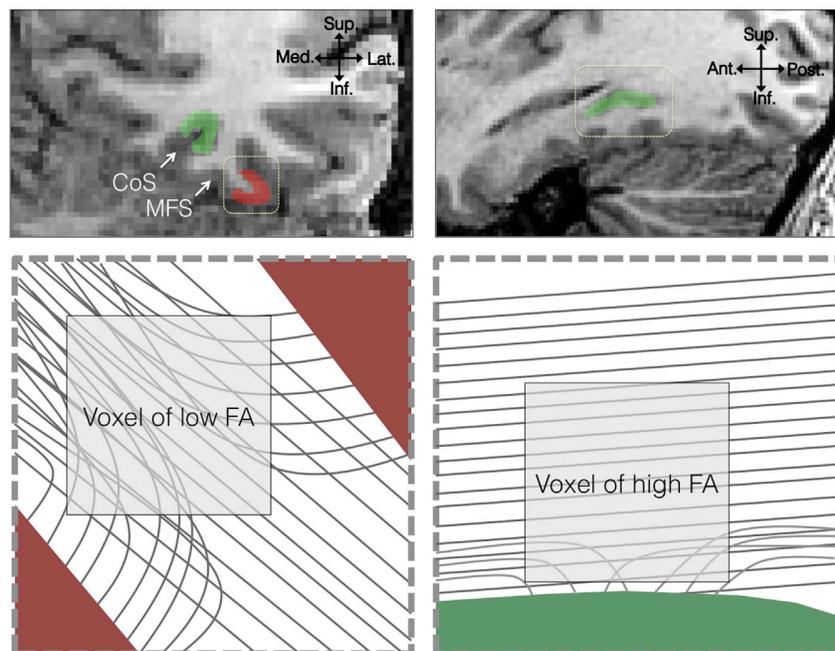


**Figure 8. Local Axonal Environment and Its Relationship to Tractography and FA**

(Upper left) A coronal section of the VTC. (Upper right) A sagittal section taken at the fundus of the collateral sulcus. Red indicates face-selective cortex on the lateral fusiform gyrus; green indicates place-selective cortex on the collateral sulcus (CoS). (Bottom left) An enlarged view of the dotted rectangle from the coronal section. Voxels within a gyrus will contain axons in multiple directions, lowering FA and making tractography near the cortical surface difficult. Increases in local connectivity to the crown of the gyrus will likely result in higher FA. (Bottom right) Enlarged view of the dotted rectangle from the sagittal slice. The fundus of the CoS is exposed to longitudinal running axons. Because these tracts are closer to cortex, increased local connectivity to cortex would lower FA.

(Figure 3), DPs presented with atypical white-matter properties in tracts associated with face-selective cortex. DPs showed restricted diffusion (lower MD) near face-selective cortex, and the FA values local to right mFus-faces showed a significantly different relationship to behavior than typical adults. This is consistent with previous research suggesting a difference in VTL white-matter properties in DP subjects relative to controls (Thomas et al., 2008). Finding an atypical relationship between FA and face processing local to mFus-faces in DP is important for two reasons. First, it demonstrates that a face-selective processing deficit is associated with atypical diffusion patterns specific to the face-processing network. Second, it provides a developmental homolog to neuropsychological findings suggesting higher rates of acquired prosopagnosia resulting from insult to occipitotemporal gray and white matter in the right hemisphere (Barton, 2008). In other words, our findings of a differential white-matter environment around mFus-faces between typical and DP adults might suggest a maldevelopment of structure-function relationships. Future research using larger sample sizes of DP subjects will be important for explicating the atypical trend we observe between white matter and face processing in DP. It is also interesting to consider if the atypical white-matter properties in DPs may affect functional or anatomical properties such as their thinner gray matter in the anterior FG compared to controls (Behrmann et al., 2007). Future studies combining novel quantitative MRI scans (Mezer et al., 2013) with DWI and fMRI will allow investigation of the interplay between connectivity, cortical characteristics, and functional properties.

### Parallel Processing Streams in Human Ventral Temporal Cortex

We found evidence for two parallel tracts in the VTL, each specifically associated with face or place processing. Notably, we

not only identified these tracts, but we also validated their existence on an independent data set using LiFE (Pestilli et al., 2014) (Figure 3B). These tracts are consistent with a local segregation model of connectivity in VTL (Figure 1B): they are inferior to the ILF, are spatially segregated near face- and place-selective regions of VTC, and partially converge in the AT lobe. While mFus-fibers and CoS-fibers are likely not the only tracts associated with mFus-faces and CoS-places, respectively, our observation of specific tracts associated with face- and place-selective cortex is consistent with prior results showing unique connectivity fingerprints for these regions (Saygin et al., 2012). The present study extends our understanding of this fingerprint by directly specifying the arrangement of connective tissue within the VTL. The existence of longitudinal mFus-fibers and CoS-fibers arranged lateral-medially and consistently with respect to the MFS (Figure 3C) mirrors the lateral-medial functional and cytoarchitectonic gradient in VTC, where the dividing boundary of these gradients aligns with the MFS (Nasr et al., 2011; Weiner et al., 2014). This suggests, in turn, that the interplay between neural hardware, connectivity, and function may determine brain networks (Tallinen et al., 2014; Van Essen et al., 1992; Witthoft et al., 2014; Zeki and Shipp, 1988).

Measurements in macaque inferior temporal cortex suggest the existence of parallel processing streams that are defined based on cortical function and white-matter connectivity (Kornblith et al., 2013; Kravitz et al., 2013), some of which form interconnected category-specific networks (Kornblith et al., 2013; Moeller et al., 2008) that may be separate from the ILF (Tusa and Ungerleider, 1985). Our finding that distinct white-matter tracts are associated with face- and place-selective cortex offers evidence that human VTL is similarly organized into multiple parallel processing streams at the level of anatomical connectivity. It would be interesting to determine in future studies if the lateral-medial arrangement of mFus-fibers and CoS-fibers tracts in humans is related to the lateral-medial topology of the

dorsolateral-inferior and ventromedial-inferior tracts identified in macaque temporal lobe with axonal tracing (Kravitz et al., 2013).

The fact that mFus-fibers and CoS-fibers are initially segregated in posterior portions and then partially overlapping in anterior regions (Figures 1B and 3A) has implications for information segregation and integration within the temporal lobe (Kravitz et al., 2013; Van Essen et al., 1992; Zeki and Shipp, 1988). Spatial separation, or divergence, provides a physical mechanism by which to parallelize the processing of independent information. In contrast, overlapping connections provide a mechanism to integrate information. We note that in the AT lobe some mFus- and CoS-fibers remain spatially separated, while others converge (Figure 3A). The former tracts are consistent with reports revealing unique connections within the face-processing network between regions in the FG and AT lobe (Moeller et al., 2008; Pyles et al., 2013). Thus, the tracts that remain spatially segregated in AT may convey network specific information, whereas the mFus- and CoS-fibers that overlap in AT may allow integration of face and place information. These hypotheses can be tested in future research combining whole-brain functional and diffusion measurements.

In sum, human ventral visual cortex relies on a network of functionally selective and intricately wired regions to produce relevant computations and functions. Our findings reveal that the functional organization of VTC is intimately coupled with patterns of white-matter connectivity. Moreover, our data indicate that this relationship supports specific visual abilities, such as face and place processing. Thus, focal disruption of the relationship between white matter and functional cortex in development may result in selective visual deficits such as DP. Future neuroimaging seeking to relate connectivity of the brain to behavior should focus on white matter defined by local cortical functions, as the present findings indicate that such fine-scale connectivity is behaviorally relevant in both health and deficit.

## EXPERIMENTAL PROCEDURES

### Participants

Eighteen typical adults ages 18–40 years (eight females, mean age  $26.4 \pm 7.1$ ) and eight adults ages 24–53 years (two females, mean age  $34 \pm 10$ ) with DP participated in this study. These adults were included as DP if they scored lower than 2 SD on the CFMT (Duchaine and Nakayama, 2006) compared to a control group of typical adult subjects matched in age ( $t(1.15) = 1.89$ ,  $p > 0.05$ ) and education (Figure S2). Subjects had normal or corrected-to-normal vision and were screened to have no prior or current neurological or psychiatric conditions. Subjects provided written informed consent prior to the experiment, and all procedures were approved to be in accordance with the Institutional Review Board of Stanford University.

### Behavioral Testing

Subjects underwent behavioral testing outside the scanner by completing the Benton Facial Recognition Test (Benton et al., 1983), an old/new scene recognition memory test (Golarai et al., 2010), and the Cambridge Face Recognition Test (Duchaine and Nakayama, 2006). Details can be found in the Supplemental Experimental Procedures.

### MRI

Nine typical adults and seven DPs were scanned on a 3-Tesla GE Signa MRI scanner at the Lucas Imaging Center, Stanford University. Another group of nine typical adults and one DP were scanned on a 3-Tesla GE scanner at the CNI, Stanford University. Whole-brain anatomicals were acquired using

a head coil using a 3D Fast SPGR scan (166 sagittal slices, resolution  $0.938 \text{ mm} \times 0.983 \text{ mm} \times 1.5 \text{ mm}$ ). Data were resampled to 1 mm isotropic voxels and aligned to the AC-PC plane. Functional MRI was obtained with a 16-channel surface coil using a T2\*-sensitive gradient echo spiral pulse sequence (Glover, 1999) with a TR = 2,000 ms, TE = 30 ms, flip angle =  $76^\circ$ , FOV = 200 mm, resolution  $3.125 \text{ mm} \times 3.125 \text{ mm} \times 3 \text{ mm}$ . We also collected inplane T1-weighted anatomicals at the same prescription as the functionals to align the data to the whole-brain volume.

### Localizer Experiment

Localizer experiment is identical to that used in our previous publication (Golarai et al., 2010). Data analysis and fROI were defined as in our prior studies (Weiner et al., 2014; Weiner and Grill-Spector, 2010); see Supplemental Experimental Procedures for details.

### Diffusion-Weighted Imaging

Nine typical adults and seven DP participants were scanned on a 3-Tesla GE Signa MRI scanner at the Lucas Imaging Center, Stanford University. We acquired two whole-brain diffusion-weighted, single-shot echo-planar imaging sequence (60 slices, TE = 80 ms, TR = 6,500 ms, 30 diffusion directions,  $b_0 = 900 \text{ s/mm}^2$ , voxel size  $2 \times 2 \times 2 \text{ mm}$ ). Each scan contained ten non-diffusion-weighted images equally distributed between diffusion-weighted images. To test the robustness of results, another group of nine typical adult and one DP participants were scanned on a 3-Tesla GE scanner at the CNI, Stanford University. We acquired two whole-brain diffusion-weighted, dual-spin echo sequences (60 slices, TE = 96.8 ms, TR = 8,000 ms, 96 diffusion directions,  $b_0 = 2,000 \text{ s/mm}^2$ , voxel size  $2 \times 2 \times 2 \text{ mm}$ ). Ten non-diffusion-weighted images were collected at the beginning of each scan. We note that changing the diffusion parameters across subject groups may affect MD, RD, or AD values, but not FA, which should stay stable. In our data there were no significant differences across groups in FA values in the mFus-fibers or ILF.

### Data Analysis

Data analysis was done using mrDiffusion (<http://white.stanford.edu/software>). Non-diffusion-weighted images were averaged, and diffusion-weighted (DW) images were registered to this mean image using a two-stage model with a coarse-to-fine approach that maximized mutual information. DWIs were motion and eddy-current corrected and aligned to each subject's whole brain anatomy using SPM8 (<http://www.fil.ion.ucl.ac.uk/spm/software/spm8/>). Tensors were fit to each voxel using a least-squares algorithm that removes outliers (Chang et al., 2005). From the tensor we calculated FA, AD, and RD (Basser and Pierpaoli, 1996).

### Tractography

We performed whole-brain white-matter tractography in one DWI data set applying a CSD model of diffusion (Tournier et al., 2007), using a probabilistic tractography algorithm implemented in the MRtrix software package (Tournier et al., 2012). Tracking used 300,000 seed points and a maximum harmonic envelope value of 6 to model for multiple crossing fibers.

### Selection and Validation of White-Matter Connectomes

LiFE (Pestilli et al., 2014) (<https://github.com/francopestilli/life>, version 0.1) was used to validate the whole-brain tractography model. After deriving a whole-brain candidate connectome from one diffusion data set, we used LiFE to build a model of the measured diffusion MRI signal given this candidate connectome. This was performed by evaluating the Stejskal-Tanner equation (Stejskal and Tanner, 1965) along the path of each individual fascicle. We employed a least-squares method to fit the LiFE model to find the contribution (weight) of each fascicle in predicting the diffusion data. False alarm fascicles, those making no contribution to the diffusion signal (zero weight), are eliminated. This procedure produces an optimized connectome with the smallest number of fascicles that best explain the diffusion data.

### The Virtual Lesion Method: Validating mFus- and CoS-fibers

After generating the LiFE-optimized connectome, we identified the mFus- and CoS-fibers in the optimized connectome. Then for each hemisphere and tract (mFus and CoS) we created two connectomes reduced to the path-neighborhood (namely, all voxels through which the tract traverses). One connectome included the tract of interest and the other excluded it—the lesioned connectome. We then computed the RMSE between the predicted and measured diffusion signals in the second data set for the lesioned and unlesioned

connectomes. Finally, we subtracted the RMSE of the unlesioned from the lesioned connectome (Figure 3B).

#### Functionally Defined White Matter

To extract white-matter tracts associated with fROIs, we generated in each subject constant-sized spheres of 6 mm radius at the center coordinate of their face- and place-fROIs. We used spheres to (1) extend fROIs to white matter to generate a seed region for tracking and (2) generate constant-sized regions to measure white-matter properties across subjects, as the size of fROIs varies across subjects. We extracted pathways from the LiFE-corrected connectome that intersected or passed within 1 mm of one fROI sphere, but not the other. To identify white-matter tracts specific to the VTL, we further restricted the fibers to those who passed through an anatomically defined plane in the AT lobe, located at the coronal slice where the frontal and temporal lobes separate. This plane is commonly used to localize fibers that have at least one terminal unique to the temporal lobe (Catani et al., 2003; Wakana et al., 2004; Yeatman et al., 2012b). Local FDWM was defined as the 10 mm segment of a FDWM tract centered above its defining fROI.

#### Defining the ILF

We used an open-source automated fasciculus extraction method (AFQ, <https://github.com/jyeatman/AFQ>) (Yeatman et al., 2012b) to define the ILF. ILF was defined as the white-matter tracts that intersected with two planes, one plane encompassing one hemisphere of the occipital lobe on a coronal slice posterior to the splenium of the corpus callosum, and the second plane the AT plane described above.

#### Relating mFus- and CoS-fibers to the ILF

In order to relate our FDWM tracts to the ILF, we first determined the ILF center using AFQ. The center is calculated as the mean of the volume (x, y, z) coordinates of all ILF fibers at each node. The spread of fibers is calculated by computing the covariance among the tracts' fibers coordinates at each node. Fibers that are more than 4 SD away from the core are not considered to be part of the tract (Yeatman et al., 2012b). We then calculated the Euclidean distance of our FDWM fibers as a function of the standard deviation of the ILF's fibers.

## SUPPLEMENTAL INFORMATION

Supplemental Information includes two figures, one table, one movie, and Supplemental Experimental Procedures and can be found with this article at <http://dx.doi.org/10.1016/j.neuron.2014.12.027>.

## ACKNOWLEDGMENTS

Thanks to Jason Yeatman for his enlightening discussions on this project, and to members of the Vision and Perception Neuroscience Lab for their feedback comments. This research was funded by NSF GRFP grant DGE-114747 to J.G. and NIH 1 RO1 EY 02231801A1 grant to K.G.-S.

Accepted: December 8, 2014

Published: January 7, 2015

## REFERENCES

- Aguirre, G.K., Zarahn, E., and D'Esposito, M. (1998). An area within human ventral cortex sensitive to "building" stimuli: evidence and implications. *Neuron* 21, 373–383.
- Allison, T., Ginter, H., McCarthy, G., Nobre, A.C., Puce, A., Luby, M., and Spencer, D.D. (1994). Face recognition in human extrastriate cortex. *J. Neurophysiol.* 71, 821–825.
- Axer, M., Grässel, D., Kleiner, M., Dammers, J., Dickscheid, T., Reckfort, J., Hütz, T., Eiben, B., Pietrzyk, U., Zilles, K., and Amunts, K. (2011). High-resolution fiber tract reconstruction in the human brain by means of three-dimensional polarized light imaging. *Front. Neuroinform.* 5, 34.
- Barton, J.J. (2008). Structure and function in acquired prosopagnosia: lessons from a series of 10 patients with brain damage. *J. Neuropsychol.* 2, 197–225.
- Basser, P.J., and Pierpaoli, C. (1996). Microstructural and physiological features of tissues elucidated by quantitative-diffusion-tensor MRI. *J. Magn. Reson. B.* 111, 209–219.
- Beaulieu, C. (2002). The basis of anisotropic water diffusion in the nervous system—a technical review. *NMR Biomed.* 15, 435–455.
- Behrmann, M., Avidan, G., Gao, F., and Black, S. (2007). Structural imaging reveals anatomical alterations in inferotemporal cortex in congenital prosopagnosia. *Cerebral Cortex* 17, 2354–2363.
- Behrmann, M., Avidan, G., Thomas, C., and Nishimura, M. (2011). Impairments in face perception. In *Oxford Handbook of Face Perception*, G. Rhodes, A. Calder, M. Johnson, and J.V. Haxby, eds. (New York: Oxford University Press).
- Benton, A., Sivan, A., Hamsher, K., Varney, N., and Spreen, O. (1983). *Contributions to Neuropsychological Assessment: A Clinical Manual*. (Oxford University Press).
- Catani, M., Jones, D.K., Donato, R., and Ffytche, D.H. (2003). Occipito-temporal connections in the human brain. *Brain* 126, 2093–2107.
- Chang, L.C., Jones, D.K., and Pierpaoli, C. (2005). RESTORE: robust estimation of tensors by outlier rejection. *Magn. Reson. Med.* 53, 1088–1095.
- De Pisapia, N., Serra, M., Rigo, P., Jager, J., Papinutto, N., Esposito, G., Venuti, P., and Bornstein, M.H. (2014). Interpersonal competence in young adulthood and right laterality in white matter. *J. Cogn. Neurosci.* 26, 1257–1265.
- Dohn, A., Garza-Villarreal, E.A., Chakravarty, M.M., Hansen, M., Lerch, J.P., and Vuust, P. (2013). Gray- and white-matter anatomy of absolute pitch possessors. *Cereb. Cortex*. Published online December 4, 2013. <http://dx.doi.org/10.1093/cercor/bht334>.
- Duchaine, B. (2011). *Developmental Prosopagnosia: Cognitive, Neural, and Developmental Investigations*. (New York: Oxford University Press).
- Duchaine, B., and Nakayama, K. (2006). The Cambridge Face Memory Test: results for neurologically intact individuals and an investigation of its validity using inverted face stimuli and prosopagnosic participants. *Neuropsychologia* 44, 576–585.
- Epstein, R., and Kanwisher, N. (1998). A cortical representation of the local visual environment. *Nature* 392, 598–601.
- Glover, G.H. (1999). Simple analytic spiral K-space algorithm. *Magn. Reson. Med.* 42, 412–415.
- Golarai, G., Ghahremani, D.G., Whitfield-Gabrieli, S., Reiss, A., Eberhardt, J.L., Gabrieli, J.D., and Grill-Spector, K. (2007). Differential development of high-level visual cortex correlates with category-specific recognition memory. *Nat. Neurosci.* 10, 512–522.
- Golarai, G., Liberman, A., Yoon, J.M., and Grill-Spector, K. (2010). Differential development of the ventral visual cortex extends through adolescence. *Front. Hum. Neurosci.* 3, 80.
- Grill-Spector, K., Knouf, N., and Kanwisher, N. (2004). The fusiform face area subserves face perception, not generic within-category identification. *Nat. Neurosci.* 7, 555–562.
- Gschwind, M., Pourtois, G., Schwartz, S., Van De Ville, D., and Vuilleumier, P. (2012). White-matter connectivity between face-responsive regions in the human brain. *Cereb. Cortex* 22, 1564–1576.
- Haskins, A.L., Yonelinas, A.P., Quamme, J.R., and Ranganath, C. (2008). Perirhinal cortex supports encoding and familiarity-based recognition of novel associations. *Neuron* 59, 554–560.
- Jbabdi, S., and Johansen-Berg, H. (2011). Tractography: where do we go from here? *Brain Connect.* 1, 169–183.
- Jones, D.K. (2008). Studying connections in the living human brain with diffusion MRI. *Cortex* 44, 936–952.
- Jones, D.K., Knösche, T.R., and Turner, R. (2013). White matter integrity, fiber count, and other fallacies: the do's and don'ts of diffusion MRI. *Neuroimage* 73, 239–254.
- Kanwisher, N., McDermott, J., and Chun, M.M. (1997). The fusiform face area: a module in human extrastriate cortex specialized for face perception. *J. Neurosci.* 17, 4302–4311.

- Kornblith, S., Cheng, X., Ohayon, S., and Tsao, D.Y. (2013). A network for scene processing in the macaque temporal lobe. *Neuron* 79, 766–781.
- Kravitz, D.J., Saleem, K.S., Baker, C.J., Ungerleider, L.G., and Mishkin, M. (2013). The ventral visual pathway: an expanded neural framework for the processing of object quality. *Trends Cogn. Sci.* 17, 26–49.
- McConachie, H.R. (1976). Developmental prosopagnosia. A single case report. *Cortex* 12, 76–82.
- McNab, J.A., Polimeni, J.R., Wang, R., Augustinack, J.C., Fujimoto, K., Stevens, A., Triantafyllou, C., Janssens, T., Farivar, R., Folkerth, R.D., et al. (2013). Surface based analysis of diffusion orientation for identifying architectonic domains in the in vivo human cortex. *Neuroimage* 69, 87–100.
- Mégevand, P., Groppe, D.M., Goldfinger, M.S., Hwang, S.T., Kingsley, P.B., Davidesco, I., and Mehta, A.D. (2014). Seeing scenes: topographic visual hallucinations evoked by direct electrical stimulation of the parahippocampal place area. *J. Neurosci.* 34, 5399–5405.
- Mezer, A., Yeatman, J.D., Stikov, N., Kay, K.N., Cho, N.J., Dougherty, R.F., Perry, M.L., Parvizi, J., Hua, H., Butts-Pauly, K., and Wandell, B.A. (2013). Quantifying the local tissue volume and composition in individual brains with magnetic resonance imaging. *Nat. Med.* 19, 1667–1672.
- Moeller, S., Freiwald, W.A., and Tsao, D.Y. (2008). Patches with links: a unified system for processing faces in the macaque temporal lobe. *Science* 320, 1355–1359.
- Moutoussis, K., and Zeki, S. (2002). The relationship between cortical activation and perception investigated with invisible stimuli. *Proc. Natl. Acad. Sci. USA* 99, 9527–9532.
- Nasr, S., Liu, N., Devaney, K.J., Yue, X., Rajimehr, R., Ungerleider, L.G., and Tootell, R.B. (2011). Scene-selective cortical regions in human and nonhuman primates. *J. Neurosci.* 31, 13771–13785.
- Parvizi, J., Jacques, C., Foster, B.L., Witthoft, N., Rangarajan, V., Weiner, K.S., and Grill-Spector, K. (2012). Electrical stimulation of human fusiform face-selective regions distorts face perception. *J. Neurosci.* 32, 14915–14920.
- Peelen, M.V., and Downing, P.E. (2005). Within-subject reproducibility of category-specific visual activation with functional MRI. *Hum. Brain Mapp.* 25, 402–408.
- Pestilli, F., Yeatman, J.D., Rokem, A., Kay, K.N., and Wandell, B.A. (2014). Evaluation and statistical inference for human connectomes. *Nat. Methods* 11, 1058–1063.
- Pyles, J.A., Verstynen, T.D., Schneider, W., and Tarr, M.J. (2013). Explicating the face perception network with white matter connectivity. *PLoS ONE* 8, e61611.
- Rangarajan, V., Hermes, D., Foster, B.L., Weiner, K.S., Jacques, C., Grill-Spector, K., and Parvizi, J. (2014). Electrical stimulation of the left and right human fusiform gyrus causes different effects in conscious face perception. *J. Neurosci.* 34, 12828–12836.
- Saygin, Z.M., Osher, D.E., Koldewyn, K., Reynolds, G., Gabrieli, J.D., and Saxe, R.R. (2012). Anatomical connectivity patterns predict face selectivity in the fusiform gyrus. *Nat. Neurosci.* 15, 321–327.
- Sporns, O., Tononi, G., and Kötter, R. (2005). The human connectome: A structural description of the human brain. *PLoS Comput. Biol.* 1, e42.
- Stejskal, E., and Tanner, J. (1965). Spin diffusion measurements: spin echoes in the presence of a time dependent field gradient. *J. Chem. Phys.* 42, 288–292.
- Tallinen, T., Chung, J.Y., Biggins, J.S., and Mahadevan, L. (2014). Gyrfication from constrained cortical expansion. *Proc. Natl. Acad. Sci. USA* 111, 12667–12672.
- Tavor, I., Yablonski, M., Mezer, A., Rom, S., Assaf, Y., and Yovel, G. (2014). Separate parts of occipito-temporal white matter fibers are associated with recognition of faces and places. *Neuroimage* 86, 123–130.
- Thomas, C., Avidan, G., Humphreys, K., Jung, K.J., Gao, F., and Behrmann, M. (2008). Reduced structural connectivity in ventral visual cortex in congenital prosopagnosia. *Nat. Neurosci.* 12, 29–31.
- Tong, F., Nakayama, K., Vaughan, J.T., and Kanwisher, N. (1998). Binocular rivalry and visual awareness in human extrastriate cortex. *Neuron* 21, 753–759.
- Tournier, J.D., Calamante, F., and Connelly, A. (2007). Robust determination of the fibre orientation distribution in diffusion MRI: non-negativity constrained super-resolved spherical deconvolution. *Neuroimage* 35, 1459–1472.
- Tournier, J.D., Calamante, F., and Connelly, A. (2012). MRtrix: diffusion tractography in crossing fibre regions. *Int. J. Imaging Syst. Technol.* 22, 53–66.
- Tusa, R.J., and Ungerleider, L.G. (1985). The inferior longitudinal fasciculus: a reexamination in humans and monkeys. *Ann. Neurol.* 18, 583–591.
- Van Essen, D.C., Anderson, C.H., and Felleman, D.J. (1992). Information processing in the primate visual system: an integrated systems perspective. *Science* 255, 419–423.
- Wakana, S., Jiang, H., Nagae-Poetscher, L.M., van Zijl, P.C., and Mori, S. (2004). Fiber tract-based atlas of human white matter anatomy. *Radiology* 230, 77–87.
- Weiner, K.S., and Grill-Spector, K. (2010). Sparsely-distributed organization of face and limb activations in human ventral temporal cortex. *Neuroimage* 52, 1559–1573.
- Weiner, K.S., Golarai, G., Caspers, J., Chuapoco, M.R., Mohlberg, H., Zilles, K., Amunts, K., and Grill-Spector, K. (2014). The mid-fusiform sulcus: a landmark identifying both cytoarchitectonic and functional divisions of human ventral temporal cortex. *Neuroimage* 84, 453–465.
- Witthoft, N., Nguyen, M.L., Golarai, G., LaRocque, K.F., Liberman, A., Smith, M.E., and Grill-Spector, K. (2014). Where is human V4? Predicting the location of hV4 and VO1 from cortical folding. *Cereb. Cortex* 24, 2401–2408.
- Yeatman, J.D., Dougherty, R.F., Ben-Shachar, M., and Wandell, B.A. (2012a). Development of white matter and reading skills. *Proc. Natl. Acad. Sci. USA* 109, E3045–E3053.
- Yeatman, J.D., Dougherty, R.F., Myall, N.J., Wandell, B.A., and Feldman, H.M. (2012b). Tract profiles of white matter properties: automating fiber-tract quantification. *PLoS ONE* 7, e49790.
- Yovel, G., Tambini, A., and Brandman, T. (2008). The asymmetry of the fusiform face area is a stable individual characteristic that underlies the left-visual-field superiority for faces. *Neuropsychologia* 46, 3061–3068.
- Zeki, S., and Shipp, S. (1988). The functional logic of cortical connections. *Nature* 335, 311–317.